Po(IV) Hydration: A Quantum Chemical Study

Regla Ayala,[†] Jose Manuel Martinez,[‡] Rafael R. Pappalardo,[‡] A. Muñoz-Paez,[†] and Enrique Sanchez Marcos*[,‡]

Departamento de Quimica Inorganica, CSIC, ICMSE, University of Sevilla, Seville 41092, Spain, and Departamento de Quimica Fisica, University of Sevilla, E-41012 Seville, Spain

Received: July 30, 2007; In Final Form: November 27, 2007

This work presents a theoretical study on the hydration of Po(IV) in solution. Three points have been addressed: (i) the level of calculation needed to properly describe the system under study, (ii) the hydration number of Po(IV), and (iii) the nature of the polonium−water bonding. The condensed medium effects have been included by means of a continuum solvation model, thus different $[Po(H_2O)_n]^{4+}$ hydrates were embedded in a cavity surrounded by a polarizable dielectric medium. Among the quantum-mechanical calculation levels here considered, the MPW1PW91 functional was shown to be the most suitable, allowing a proper description of the Po−H_2O interactions at affordable cost. The hydration number of Po(IV) was found to be between 8 and 9. This value is ruled by a dynamic equilibrium involving the octa- and ennea-hydrates, although the 7-fold coordination cannot be completely excluded. The hydration free energy of Po(IV) is estimated to be around −1480 kcal/mol. The Po−H_2O bonding is dominated by strong electrostatic contributions although a small covalent contribution is responsible for the peculiar arrangement adopted by the smaller hydrates ($n \leq 5$). A natural bond order (NBO) analysis of the hydrate wave functions shows that the covalent bond involves the empty 6p orbitals of the polonium ion and one lone pair on the oxygen atom of the water molecule. A parallel investigation to the hydrate study, where the polonium ion was replaced by a tetravalent point charge plus a repulsion potential, was carried out. These results allowed a detailed examination of the electrostatic and nonelectrostatic contributions to the polonium hydrate formation.

1. Introduction

Although the discovery of the polonium element was made by Marie Curie[1] more than one century ago, the chemistry and properties of this element and its complexes are still barely known, primarily because of two reasons. First, polonium is a very rare element in nature, being found in uranium ores at about 100 micrograms per metric ton. Second is that polonium is highly toxic,[2] the main hazard being its intense radioactivity (as an α emitter), which makes it very difficult to handle safely. Polonium has 25 known isotopes, all of them being radioactive. The half-life of ^{210}Po, the most widely available, is 138.376 days. Even at trace concentrations, this isotope is lethal by ingestion or inhalation. In the case of individual or environmental contamination, the nature of chemical species that are present are far from being understood. Therefore, characterization and understanding of polonium complexes can help to develop protocols and strategies to minimize its lethal effects on living beings, and to control its diffusion in natural environments.

Although it is known that polonium metal salts dissolve readily in dilute acids and are only slightly soluble in alkalis,[3] their chemistry in solution has scarcely been studied. In this work, we have focused on the theoretical study of the hydration of Po(IV). The absence of previous studies on this subject, either experimental or theoretical, compelled us to begin this study with the most basic of steps, the only information having been reported so far being that the hydration number of the Po(IV) in solution is between 6 and 8.[4] The use of computational chemistry can increase our understanding of these systems while avoiding the difficulties of experimental methods. Since a standard methodology to achieve an accurate description of ionic solvation phenomena has not been established, the first chemical candidates to be thoroughly examined were the aquaion forms, $[Po(H_2O)_n]^{4+}$. These species should be present in highly acidic aqueous solutions, as reported for other tetravalent cations in similar media.[5,6]

Taking into account the high charge of this radioactive cation, several species such as aquaions, hydrolyzed forms or oligomers, may be expected in aqueous solutions as a function of the medium acidity, ionic strength, the presence of counterions, and other factors. Therefore, considering this complex scenario, we have focused exclusively on the aquaion forms.

To unveil the nature of ionic solutions from the computational point of view, it is essential to gain knowledge of the structural, thermodynamic, and dynamical properties of the system under study. Considering first the structural and thermodynamic properties, the study of small clusters $[M(H_2O)_n]^{m+/-}$ (n typically between 1 and 10) in gas phase and the a posteriori inclusion of bulk solvent effects via the polarizable continuum model (PCM)[7] can give us an initial guide to the behavior of the system in solution.[8−10] To get further insight into the system it is necessary to perform computer simulations, e.g., Monte Carlo or molecular dynamics. These methods require the availability of reliable interaction potentials for classical simulations or pseudopotentials and/or basis sets for ab initio simulations.

This work focuses on the structural and thermodynamic properties of the Po(IV) in aqueous solution. The strategy applied has been the analysis of both the specific Po−H_2O

* Corresponding author.E-mail: sanchez@us.es.
[†] Departamento de Quimica Inorganica.
[‡] Departamento de Quimica Fisica.

10.1021/jp076032r CCC: $40.75
Published on Web 04/09/2008

interactions in $[Po(H_2O)_n]^{4+}$ clusters with an increasing number of water molecules, as well as the analysis of long-range interactions with the bulk by including a dielectric continuum surrounding the aquaions.

The aim of this work is centered on three points. The first one is to find a reasonable quantum mechanical level involving the inclusion of solvent effects to tackle the Po(IV) hydration. The second is the determination of the most stable structure for the aquaion, while the third is the description of the bonding nature of the polonium hydrates.

2. Methodology

Ab initio (HF, MP2, and CCSD(T)) and density functional theory (DFT) (B3LYP,[11,12] G96LYP[13−16] and MPW1PW91[17]) methods were used to optimize $[Po(H_2O)_n]^{4+}$ clusters in gas phase for $n = 1-9$, and for CCSD(T) $n = 1-3$. Calculations were carried out with the Gaussian 03 program,[18] except for the CCSD(T) calculations, which were performed with the NWCHEM program.[19] Although hybrid functionals are generally considered more suitable for transition metal chemistry,[20,21] G96LYP was also included in this work on the basis of Truhlar and co-workers results.[22,23] The Dunning aug-cc-pVDZ[24] basis sets were used for O and H. For Po, the relativistic small core pseudopotential (60 core electrons) developed by Dolg and co-workers[25] was used for the core electrons, while the valence electrons were described with the aug-cc-pVDZ basis set.[25] The choice of Dunning basis sets was motivated by the desire for consistency with the limited availability of high quality small core pseudopotentials and basis sets for the polonium atom.

In the first instance, the $[Po(H_2O)_n]^{4+}$ ($n = 1-9$) clusters were fully optimized in gas phase. Different optimizations starting from usual arrangements corresponding to each coordination number were performed. In the case of clusters with $n = 1-6$, the final structures are shown in Figure 1. For larger clusters ($n = 7-9$), depending on the starting geometry, we obtained either the optimized geometries given in Figure 1 or structures where a rearrangement of the first hydration shell had taken place, in conjunction with the migration of some water molecules to the second hydration shell. The explicit hydration beyond the first shell is out of the scope of this study and would need a different methodological framework.[33]

The basis set superposition error (BSSE) was computed using the counter-poise method[26,27] for $[Po(H_2O)_n]^{4+}$ clusters with $n = 1$ and 2. For the DFT methods, the estimation of the BSSE was smaller than 0.2% of the total energy, whereas values below 2% were obtained for the MP2 and CCSD(T) methods. The $[Po(H_2O)_n]^{4+}$ ($n = 1-9$) clusters that were characterized as minima (no negative frequencies) were taken as the starting point for the optimizations in solution via the polarizable continuum method in the integral equation formalism (IEFPCM).[28−31] The continuum-discrete model used in this study takes into account the cavity containing the Po(IV) ion and its first hydration shell, and the dielectric continuum surrounding the cavity.[8,10] The static dielectric permittivity of liquid water at 298 K ($\epsilon = 78.39$) was used for the dielectric continuum. With the reoptimization in solution, bulk solvent effects were taken into account on both energies and geometries. As shown in a number of previous studies of monatomic cations, the inclusion of explicit solvent molecules in the first hydration shell is necessary to obtain reliable values of the free energy of solvation.[8,32] The second or outer solvation shells are rarely included due to the rapid increase of computational cost, as well as methodological concerns associated with proper inclusion of statistical contributions in the quantum mechanical calculations.[33,32] The cavity

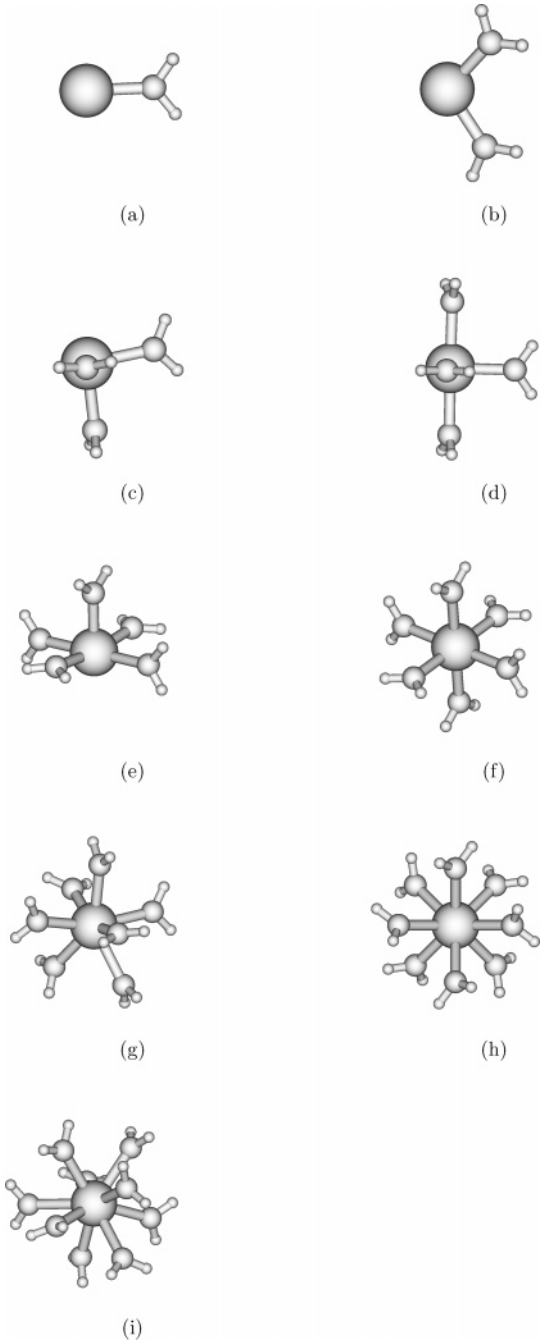

Figure 1. MPW1PW91 optimized structures of $[Po(H_2O)_n]^{4+}$ clusters ($n = 1-9$).

enclosing the hydrates was built using the following radii: 1.520 Å for O, 1.200 Å for H, and 2.354 Å for Po.[34,35] These radii have been multiplied by a standard factor of 1.2 in order to take into account the fact that atomic bond or lone pair centers of the solvent molecules are normally located slightly further from the solute atoms than their van der Waals radii.[7] Free energies of the clusters in gas phase and in solution were calculated.

Solvation free energies were calculated within the semi-continuum model[33,36,37] as

$$\Delta G_{solv} = \Delta G_{cluster} + \Delta G_{cont} + \Delta G_{cav} + \Delta G_{disp-rep} + n\Delta G_{vap} \quad (1)$$

where $\Delta G_{cluster}$ is the free energy of formation of the cluster; ΔG_{cont} is the solvation energy corresponding to the long-range

interactions of the hydrated cluster embedded in a cavity inside a continuum; ΔG_{cav} is the free energy needed to create the cavity; $\Delta G_{disp-rep}$ is a term that collects the hydrate-continuum dispersion and repulsion contributions; and $n\Delta G_{vap}$ is the free energy needed to evaporate n water molecules from the liquid pure solvent to the gas phase, in order to form the hydrate. A temperature of 298 K was assumed. As previously reported,[9,10,33,38] the standard application of the PCM method using the interlocked spheres procedure to define the solute cavity predicts a shortening of the Po−O distance in the $[Po(H_2O)_n]^{4+}$ hydrate compared to the gas-phase geometry. In our case, this shortening is about 0.05 Å. However, $\Delta G_{cluster}$ was computed from the gas-phase geometries because the shortening due to solvent effects has an almost negligible energetic effect (less than 5 kcal/mol in all cases). The polonium contribution to the dispersion and repulsion term was neglected, as no parameters are currently available for that element. Nevertheless, the dispersion−repulsion term of the hydrate is largely dominated by the first hydration shell where water molecules roughly enclose the polonium cation, making its contribution negligible. ΔG_{vap} was taken from experimental data (2.05 kcal/mol).[39]

3. Results and Discussion

3.1. Choice of Calculation Level. In order to ascertain the most convenient computational methods to properly describe $[Po(H_2O)_n]^{4+}$ clusters, different ab initio (HF, MP2, CCSD(T)) and DFT (B3LYP, G96LYP, MPW1PW91) methods were tested. In the absence of experimental data, we assumed that an accurate description of energetics and structural properties of the Po−H_2O clusters would be given by high-level ab initio calculations such as CCSD(T). This method is generally regarded as the most accurate among the electronic structure methods practically applicable.[40] The excellent agreement between CCSD(T) and experimental results for other molecular systems supports the hypothesis that this level of theory will predict accurate properties such as bonding distances and interaction energies.[41,42] However, while CCSD(T) calculations are highly accurate, they are computationally too expensive and cannot be used for full geometry optimizations of clusters with $n > 3$. This is mainly due to the fact that the gradients required for the optimization have to be computed numerically. For instance, the full geometry optimization of the $[Po(H_2O)_3]^{4+}$ cluster at CCSD(T) level took 20 days using 8 Itanium 2 1.6 GHz CPUs. Nevertheless, results for the small clusters optimized at the CCSD(T) level can be used as a reference to calibrate the other methods included in this study.

Table 1 shows structural data for the methods and clusters considered in this work. The equilibrium structures for the $[Po(H_2O)_n]^{4+}$ clusters ($n = 1-9$) obtained by the MPW1PW91 method are shown in Figure 1. The optimizations carried out with HF, MP2, CCSD(T), and B3LYP generate similar structures. G96LYP-optimized structures for $n = 3-5$ are slightly different. The main differences in the results obtained by the different methods employed are found in the Po−O distances. As a rule, DFT Po−O distances are longer than ab initio ones, the gap with HF and MP2 being more pronounced than that for CCSD(T). The longest distances are obtained with G96LYP, whereas B3LYP and MPW1PW91 are more similar to each other and to ab initio methods. As expected, Po−O distances lengthen with the increase of the hydration number for all computational levels. A closer analysis of Table 1 shows that there is not a simple pattern defining the Po−O distance in terms of the number of water molecules, n, and the method employed. For $n = 1$ CCSD(T), the Po−O distance is closer to the B3LYP distance than to those of the other two DFT methods (MPW1PW91 and G96LYP), while it is longer than both the HF and MP2 distances. For $n = 2$, CCSD(T) Po−O distances are more similar to those of MPW1PW91 than to those of the other methods. HF and MP2 Po−O distances reduce their discrepancies with CCSD(T). B3LYP Po−O distances are slightly longer than those obtained from CCSD(T), while the G96LYP distances are too long. The results for $n = 3$ follow the trend shown for $n = 2$, that is, CCSD(T) and MPW1PW91 distances are similar, HF and MP2 results evolve to resemble CCSD(T) ones, B3LYP Po−O distances are slightly longer than CCSD(T) results, and G96LYP results are too long.

TABLE 1: Po−O Distances (Å) of the $[Po(H_2O)_n]^{4+}$ Clusters ($n = 1-9$) Optimized by Different Quantum Mechanical Methods

n	HF	MP2	MPW1PW91	B3LYP	G96LYP	CCSD(T)
1	2.05	2.08	2.10	2.12	2.18	2.13
2	2.08	2.11	2.12	2.15	2.19	2.12
3	2.12	2.14	2.15	2.18	2.21	2.15
4	2.13	2.15	2.17	2.19	2.30	
	2.14	2.16	2.18	2.21		
	2.23 × 2	2.25 × 2	2.26 × 2	2.28 × 2		
5	2.13	2.15	2.17	2.20	2.30	
	2.26 × 4	2.27 × 4	2.28 × 4	2.30 × 4	2.33 × 3	
					2.34	
6	2.30	2.30	2.31	2.33	2.36	
7	2.31	2.31 × 3	2.32 × 2	2.34 × 2	2.37 × 2	
	2.32 × 2	2.35 × 3	2.36 × 2	2.35	2.38	
	2.35 × 2	2.36	2.37	2.38 × 2	2.41 × 2	
	2.39		2.38 × 2	2.40 × 2	2.43 × 2	
8	2.38	2.37	2.38	2.40	2.44	
9	2.40 × 6	2.39 × 6	2.40 × 6	2.42 × 6	2.45 × 3	
	2.47 × 3	2.45 × 3	2.46 × 3	2.49 × 3	2.47 × 3	
					2.54 × 3	

The previous analysis of the results obtained for $[Po(H_2O)_n]^{4+}$ clusters ($n = 1-3$) highlights a difference in the results of the methods between G96LYP, where the results diverge from CCSD(T), and the other methods, HF, MP2, MPW1PW91, and B3LYP, where results resemble those from CCSD(T) to a certain extent. Although CCSD(T) results are not available for $n \geq 4$, results from the other methods can be compared to each other, and they show that the trend observed in the small clusters ($n = 1-3$) is maintained. HF, MP2, MPW1PW91, and B3LYP results are more similar as n increases, especially in the case of the first three methods, while G96LYP distances are consistently longer.

Not only does G96LYP overestimate Po−O distances, but also the structures for clusters with $n = 3-5$ were observed to be slightly different. As shown in Figure 1c, in other cases the $[Po(H_2O)_3]^{4+}$ cluster is not flat but adopts a trigonal pyramid arrangement. This pyramidalization is less marked in the case of G96LYP. For $n = 4$, the cluster optimized at G96LYP can be described as a distorted tetrahedron centered on the polonium atom, while the remaining structures followed the arrangement shown in Figure 1d. This structure (Figure 1d) is peculiar since it is rather different from the typical arrangements for this coordination, either tetrahedral or square planar coordination with the cation in the center. The origin of this peculiar structure (Figure 1d) and the nature of the Po−H_2O bonding will be discussed in section 3.3. A singular behavior of G96LYP in the structural pattern of the water molecules around the polonium ion is again found for $n = 5$. In this sense, whereas $[Po(H_2O)_5]^{4+}$ structures optimized by HF, MP2, MPW1PW91, and B3LYP methods can be defined as distorted tetragonal pyramids centered on the metal cation (Figure 1e), the G96LYP structure is a distorted trigonal bipyramid in which the ion is at the center. For $n = 6-9$, the structures are pretty similar, regardless of the

TABLE 2: Interaction Energies, E_{int} (kcal/mol), of the Optimized $[Po(H_2O)_n]^{4+}$ Structures ($n = 1-9$) Obtained by Different Quantum Mechanical Methods

n	HF	MP2	MPW1PW91	B3LYP	G96LYP	CCSD(T)
1	−218.3	−238.8	−249.7	−253.1	−261.5	−239.1
2	−388.1	−417.7	−434.9	−437.9	−426.1	−415.7
3	−522.7	−554.1	−572.4	−572.8	−545.2	−550.1
4	−614.7	−650.7	−669.6	−669.2	−631.4	-
5	−694.7	−735.6	−753.6	−751.9	−697.9	-
6	−759.5	−807.4	−825.8	−823.8	−754.6	-
7	−808.9	−860.2	−874.5	−870.8	−784.3	-
8	−855.2	−910.9	−920.4	−885.5	−811.6	-
9	−915.2	−946.6	−951.0	−944.7	−823.9	-

method, although G96LYP distances are in all cases longer than those obtained with the other methods. A cluster for $n = 10$ bearing all the water molecules in the first hydration shell cannot be optimized. Irrespective of the starting structure or method, one or more water molecules were expelled from the first hydration shell of the Po(IV), leading to octa- or ennea-hydrates.

Table 2 shows the interaction energies, E_{int}, for the $[Po(H_2O)_n]^{4+}$ clusters ($n = 1-9$) at different levels of calculation. The interaction energy increases with the number of water molecules, but, because of many body effects, the energy per water molecule is reduced when going from small to large clusters. This behavior runs parallel to the elongation of the Po−O distance with n as observed in Table 1. For $n = 1$, CCSD(T) E_{int} (−239.1 kcal/mol) is close to the MP2 one (−238.8 kcal/mol), while DFT methods over-stabilize the polonium−water interaction (E_{int} is −249.7, −253.1, and −261.5 kcal/mol for MPW1PW91, B3LYP, and G96LYP, respectively). The value of E_{int} for the HF method (−218.3 kcal/mol) is an underestimate of the value obtained through CCSD(T) methods. For $n = 2-3$, MP2 provides interaction energies very similar to the CCSD(T) ones, followed closely by G96LYP, MPW1PW91 and B3LYP. HF again underestimates CCSD(T) results. On the basis of these results, HF can be ruled out for the purpose of this study. As n increases, the interaction energy per water molecule and, consequently, the total interaction energy is very similar for the MP2, MPW1PW91, and B3LYP methods. In the case of MP2 and MPW1PW91, they are almost identical for larger values of n. However, G96LYP begins with the most attractive interaction per water molecule and ends up with the least attractive character. It seems that many body effects are more important with G96LYP than in the other methods. On the basis of the structural and energetic results of this study, it seems that the larger n is, the more similar MP2 and MPW1PW91 results are. Recalling that CCSD(T) results are our reference, we have on one hand that MPW1PW91 structures resemble the CCSD(T) ones, and on the other hand, MP2 interaction energies are similar to the CCSD(T) values. MPW1PW91 appears to be the most suitable method since it is less CPU time demanding than MP2, and a compromise between accuracy and feasibility is desirable.

3.2. Semi-continuum Solvation Model. To study the combined effect of specific and long-range solvent effects, we have selected a set of larger clusters, with a number of water molecules high enough to completely surround the central cation. Thus, the semi-continuum model treats each hydration region at the same methodological level. This would not be the case if clusters with a smaller number of molecules were considered (the extreme case would be $n = 1$) because part of the first hydration shell would have been described by the discrete model and the rest by the continuum one. Examination of the solvation data given in Table 3 reveals that the solvation energy contribution depends on cluster size. Although the nonelectrostatic contributions ΔG_{cav} and $\Delta G_{disp-rep}$ depend on the cluster volume, their sum is a minor contribution to ΔG_{solv} because there is a significant cancellation between them. The formation energy of the cluster, $\Delta G_{cluster}$, and the continuum contribution, ΔG_{cont}, present more significant changes, although, as expected, the trend with the increase in the cluster size is in the opposite direction. $\Delta G_{cluster}$ becomes more stabilizing (more negative) when the number of water molecules directly attached to the metal cation increases, while ΔG_{cont} is less stabilizing (less negative) when the cavity size increases, i.e., when the cluster is larger.

TABLE 3: Solvation Free Energy ΔG_{solv} (kcal/mol) and Its Components for the MPW1PW91 Clusters Including Solvent Effects via PCM Model[a]

n	cavity volume[b]	$\Delta G_{cluster}$	ΔG_{cont}	$n\Delta G_{vap}$[c]	$\Delta G_{cav+dis-rep}$	ΔG_{solv}
6	190.6	−762.9	−708.7	12.3	10.4	−1448.9
7	209.5	−800.8	−691.3	14.4	11.9	−1465.8
8	230.4	−831.9	−674.8	16.4	14.2	−1476.1
9	248.9	−851.5	−660.6	18.4	14.2	−1479.5

[a] $\Delta G_{cluster}$ was computed from the gas-phase structure. [b] Cavity volume in Å^3. [c] Experimental value of ΔG_{vap} was taken from ref 39.

The lack of experimental data precludes the direct validation of our results. However, the comparison of our results with experimental data of other tetravalent cations such as Zr^{4+}, Sn^{4+}, Ce^{4+}, Hf $^{4+}$, Th^{4+}, Pa^{4+}, U^{4+}, Np^{4+}, and Pu^{4+} indicates that our estimation for the hydration free energy (−1479.5 kcal/mol) is within the range of values obtained for this set of cations [1380−1800] kcal/mol.[5] Moreover, Po−O distances (2.1−2.5 Å) are also in agreement with the experimental results of tetravalent cations in aqueous solutions [2.22−2.51 Å].[4,6,43]

The $[Po(H_2O)_9]^{4+}$ cluster seems to be the most stable one in solution. However, the energy difference with the $[Po(H_2O)_8]^{4+}$ one is negligible, especially taking into account that the uncertainty associated with this theoretical procedure of estimating ΔG_{solv} may be quantified as a 5−7% of the absolute value.[33,44] When comparing ΔG_{solv} within a series, the uncertainty associated with the energy gap ($\Delta\Delta G_{solv} = \Delta G_{solv,1} - \Delta G_{solv,2}$) decreases because there is cancellation of common contributions. Then, $\Delta\Delta G_{solv}$ values of the hydrates are affected roughly by 1.5%, that is, ∼20 kcal/mol. We can conclude that on the basis of our study, the hydration number of the Po(IV) is ruled by a dynamic equilibrium involving the octa- and ennea-hydrates, although a 7-fold coordination cannot be completely excluded. This indicates the existence of a region in the potential energy surface with several minima close in energy. The intrinsic dynamic behavior of this equilibrium implies, for a complete description, the use of further computer simulations where an appropriate statistical average is accounted for.

3.3. Bond Analysis and Point Charge Calculations. To complete the description of ion hydration, in addition to the estimation of solvation free energies and hydration numbers, a detailed description of the nature of the ion−solvent bonding must be supplied. In Figure 1, the five smaller $[Po(H_2O)_n]^{4+}$ ($n \leq 5$) clusters can be labeled as surface clusters, denoting that the ion is exposed and not completely buried in the center of the cluster. In the case of clusters with $n \leq 3$, this could be understood because the number of water molecules is not large enough to completely surround the ion. Nevertheless, for $n = 4-5$, the distribution pattern of water molecules around the ion is not that expected for a tetravalent cation, that is, the water molecules symmetrically distributed around the ion, maximizing the ion−solvent interactions and minimizing solvent−solvent repulsions at the same time. Obviously, the distribution of water

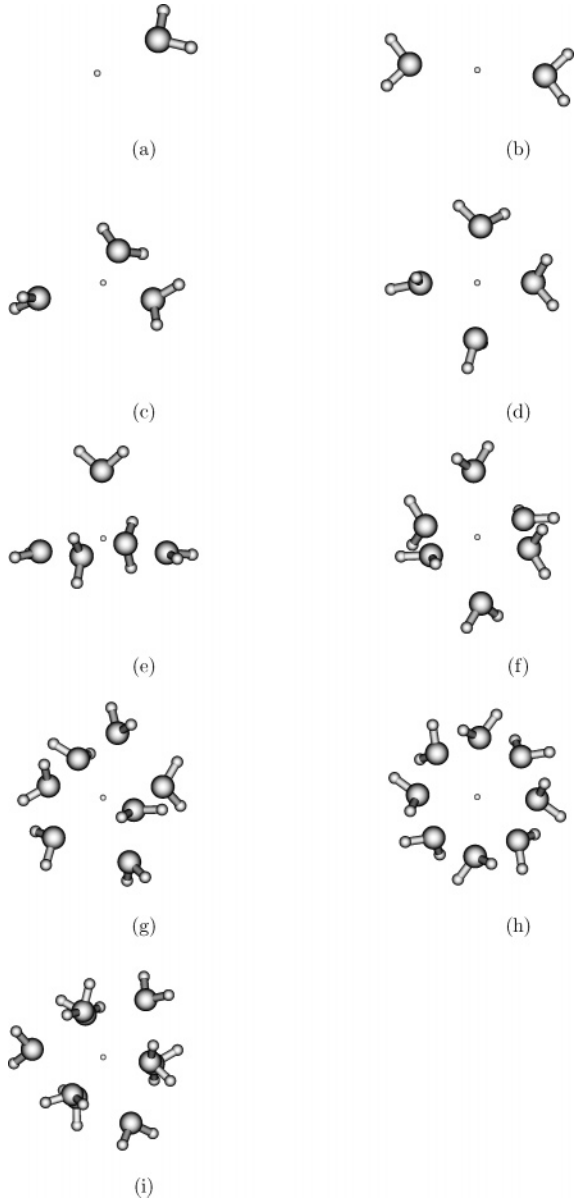

Figure 2. MPW1PW91 optimized structures of $[q-(H_2O)_n]^{4+}$ clusters ($n = 1-9$).

molecules in these clusters is not the optimum from the point of view of water−water repulsions. In order to understand the reasons of this unusual structural arrangement, it is necessary to analyze the driving force of the Po−H_2O interaction. A natural bond order (NBO) analysis[45] of the $[Po(H_2O)_n]^{4+}$ clusters with $n = 1-7$ shows that there is covalent bond formation between the 6p orbitals of polonium ion and the water molecules, without a significant participation of the 6s orbital of the polonium ion in the bonding. For $n = 8$ and 9, the NBO analysis indicates the participation of the 6d orbitals of the polonium ion in the bonding, but not of the 6s orbital. In practice, the polonium 6s orbital may be considered a core orbital. Figure 3 shows a 3D plot of the three localized natural Po−O bonding molecular orbital in $[Po(H_2O)_3]^{4+}$, as derived from an NBO analysis. It is seen that the O−Po−O angle is ~90° in all cases. Figure 4 illustrates how the increase in the number of water molecules involved in the Po(IV) cluster formation leads to the saturation of the bonding capability of the 6p Po orbital, this bonding behavior being responsible for the observed final structures. This way, O−Po−O angles in the $[Po(H_2O)_n]^{4+}$ cluster ($n = 2-6$) are around 90 or 180° as a

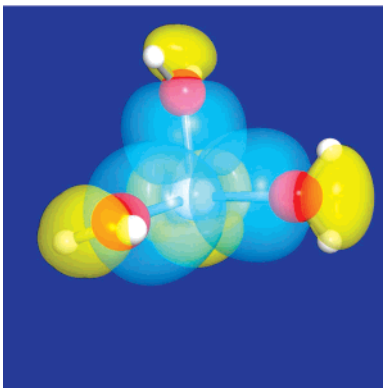

Figure 3. 3D representation of the three natural Po−O bond molecular orbitals of the $[Po(H_2O)_3]^{4+}$ cluster obtained with NBOView.

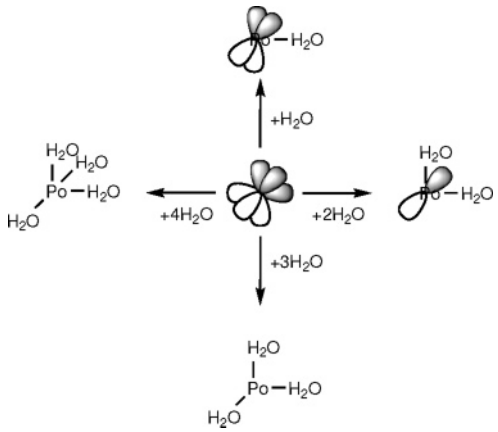

Figure 4. Schematic representation of how the Po(IV) cation and water molecules interact through the 6p Po orbitals for the $n = 1-4$ clusters.

result of the interaction of the water molecules with the 6p orbitals of the polonium ion. The lack of hybridization between the 6p and 6s polonium orbitals precludes the formation of small clusters with water molecules symmetrically distributed around the ion. This simple model is capable of explaining water arrangements in the polonium hydrates and underlines the importance of the directionality imposed by the covalent contribution of the ion−solvent interactions in the final $[Po(H_2O)_n]^{4+}$ ($n = 1-5$) structures. Despite the fact that there is a certain covalent bonding between the polonium ion and the water molecules, the natural population analysis indicates that the electron donation from a water molecule of the cluster to the positively charged ion is between 0.48*e* ($n = 1$) and 0.16*e* ($n = 9$). Bearing in mind that we are dealing with a tetravalent cation, the charge transfer from water molecules to the ion is small. This suggests that electrostatic attraction should play a major role in the total stabilization of complex formation for the Po−H_2O clusters.

To quantify the electrostatic and its associated long-range contributions to Po−H_2O interaction, we compared the results of the $[Po(H_2O)_n]^{4+}$ clusters with those resulting from the optimization of *n* water molecules plus a 4+ point charge (q^{4+}) at the MPW1PW91 level. In these calculations, the diffuse functions on the O and H were eliminated due to convergence difficulties of the SCF process. To avoid the collapse of the water molecules with the point charge, a classical pair potential of the form $A \cdot e^{-r/B}$ ($A = 530$ a.u., $B = 0.47$ Å, and r is the q^{4+}−O and q^{4+}−H distances in Å) was applied at the charge site. These parameters were chosen in such a way that the Po−O distances of the optimized $[Po(H_2O)_6]^{4+}$ hydrate were reproduced. By this procedure, the size of the polonium ion was to

TABLE 4: MPW1PW91 Interaction Energy of the Polonium Ion with Water Molecules, $E_{int_{Po}}$, in $[Po(H_2O)_n]^{4+}$ Clusters (n = 1−9) and Interaction Energy of a 4+ Point Charge (q) with Water Molecules, E_{int_q}, for $[q^{4+}-(H_2O)_n]$ Clusters (n = 1−9) Including a Classical Pair Potential (see text).[a]

n	$E_{int_{Po}}$	E_{int_q}	$(E_{int_{Po}} - E_{int_q})/n$
1	−269.2	−179.1	−90.1
2	−460.4	−344.0	−58.2
3	−604.0	−491.2	−37.6
4	−709.8	−623.0	−21.7
5	−803.0	−724.7	−15.7
6	−885.5	−821.4	−10.7
7	−947.2	−864.0	−11.9
8	−1006.1	−914.3	−11.5
9	−1053.9	−948.1	−11.8

[a] Comparison of the difference between $E_{int_{Po}}$ and E_{int_q} per water molecule ($[E_{int_{Po}} - E_{int_q}]/n$)) has been included in the third column. (All energies are in kcal/mol.)

a certain extent also reproduced. This type of computation could be envisaged as a molecular mechanics/quantum mechanics (MM/QM) computation in the sense that there is a lower level of computation in the key part of the system: the polonium ion, which plays a central role in our study, was described by a point charge and the pair potential (MM), whereas the water molecules were described quantum mechanically (QM). The results are shown in Figure 2 and Table 4. For $n = 5-9$ the final $q^{4+}-H_2O$ structures are very similar to those obtained in the optimization process of $[Po(H_2O)_{5-9}]^{4+}$ clusters. Even the unexpected arrangement of the $[Po(H_2O)_5]^{4+}$ clusters in which four water molecules are in the same plane of the ion increasing the steric effect among them is well reproduced. However, the results for $n = 1-4$ show discrepancies with the optimized $[Po(H_2O)_{1-4}]^{4+}$ clusters. For $n = 4$ (Figure 2d), the structure is very similar to the one optimized with G96LYP, that is, a tetrahedron with the ion in the center. An NBO analysis of the G96LYP optimized $[Po(H_2O)_4]^{4+}$ cluster indicates that in addition to the 6*p* orbitals, the 6*s* orbital of the polonium ion is also participating in the polonium ion−water bond. This result is contrary to MPW1PW91 NBO analysis where only the 6p orbitals were involved in the bonding, and it is responsible for the differences between the structures obtained at the G96LYP level and the rest of the methods considered in this study. For $n = 3$ (Figure 2c) and 2 (Figure 2b), the point charge clusters are flat and linear, respectively, minimizing the repulsion among the water molecules, whereas the $[Po(H_2O)_n]^{4+}$ clusters with $n = 3$ (Figure 1c) and 4 (Figure 1d) are bent and pyramidal, respectively, as previously discussed.

Table 4 displays the interaction energies, $E_{int_{Po}}$ and E_{int_q}, corresponding to the $[Po(H_2O)_n]^{4+}$ and $[q(H_2O)_n]^{4+}$ clusters, respectively. These values give the interaction energy between the central ion (either Po(IV) or q^{4+}) and the water aggregate by using the following expressions:

$$E_{int_{Po}} = E_{[Po(H_2O)n]^{4+}} - E_{(H_2O)n} - E_{Po^{4+}}$$

$$E_{int_q} = E_{[q^{4+}-(H_2O)n]} - E_{(H_2O)_n} - E_{MM}$$

where E represents the total quantum-mechanical energy of the different chemical systems, and E_{MM} represents the contribution due to the pair potential associated to q^{4+}. From $n = 6-9$, the difference between E_{int_q} and $E_{int_{Po}}$ amounts to ∼11 kcal/mol per water molecule. Nevertheless, this value is not constant for $n = 1-5$. This discrepancy between small ($n = 1-5$) and large clusters ($n = 6-9$) might be ascribed to the fact that the pair potential applied was fitted to reproduce the $[Po(H_2O)_6]^{4+}$ cluster. Changing A and B parameters of the pair potential to reproduce the Po−O distances for $n = 2$, the same arrangement is found, although Po−O distances were shorter as a consequence of the fact that the hydrate pattern used for the fitting shows smaller cation−water distances (cf. $n = 2$ vs $n = 6$ in Table 1). This result ignores the fact that the choice of the parameters is responsible for the discrepancies between point charge−water and Po(IV)−water clusters for $n = 1-4$. Bearing in mind the previous NBO analysis, the discrepancies in both interaction energy and structure can be explained in terms of the bonding nature. For smaller clusters ($n = 1-3$), the bonding between the polonium ion and the water molecules is stronger since only one water molecule is interacting with each of the 6p orbitals. However, when n increases, the covalent bonding contribution becomes smaller because more than one water molecule is interacting with each of the 6p orbitals at the same time. This behavior is reflected in Table 4. When all three 6p orbitals are interacting with at least two water molecules, the difference between E_{int_q} and $E_{int_{Po}}$ is almost constant per water molecule. The differences between E_{int_q} and $E_{int_{Po}}$ are due to the stabilizing bonding component in the $Po-H_2O$ clusters that is not present in the $q^{4+}-H_2O$ ones.

The different structures adopted by the small size clusters ($n = 1-4$), where the polonium ion is replaced by the point charge, confirm the importance of the covalent bonding in determining the Po(IV) hydrate geometries. Although orbital interaction is responsible for the structure of the clusters, the electrostatic and its associated long-range contributions retain most of the $Po-H_2O$ interaction energy, especially in the case of larger clusters, where it is around 90% of the total interaction energy, which reduces to ∼67% to 75% for the mono and dihydrate.

4. Concluding Remarks

In this work, we have investigated the structural and thermodynamic properties of the Po(IV) cation in aqueous solution. We have focused on the aquaion species, although we are aware that the high charge of the polonium ion along with the conditions of the medium can give rise to different species, such as hydrolyzed forms, which will be studied in a second work. On the basis of gas-phase results for $[Po(H_2O)_n]^{4+}$ clusters at different levels of calculation, we conclude that MPW1PW91 is the most suitable method, among the ones here considered, to describe properly the nature of the Po−water bond. The properties in solution have been studied using a combined discrete-continuum approach; specific ion−solvent interactions were described quantum-mechanically, and long-range interactions were introduced by the IEFPCM model. Structural reoptimization of the $[Po(H_2O)_n]^{4+}$ clusters in a cavity leads to a shortening of the Po−O distance by about 0.05 Å. We conclude that the hydration number of the Po(IV) is ruled by a dynamic equilibrium mainly involving the hepta-, octa-, and ennea-hydrates, and the solvation free energy is around −1480 ± 70 kcal/mol. Concerning the nature of the $Po-H_2O$ bonding, it has been shown that orbital interaction between the 6p orbitals of the polonium ion and the water molecules is responsible for the structure of the smaller clusters. However, the electrostatic and its associated long-range contributions are responsible for most of the energetics of the $Po-H_2O$ interaction, especially in the case of larger clusters.

Acknowledgment. Spanish DGICYT (CTQ2005-03657) and Junta de Andalucia (P06-FQM-01484) are acknowledged for financial support. We thank Dr. C. Domene, University of

Oxford, for careful revision of the manuscript. R.A.E. thanks Spanish CSIC for a postdoctoral I3P fellowship.

References and Notes

(1) Curie, P.; Curie, M. P. *Comptes Rendus* **1898**, *127*, 175.
(2) Harrison, J.; Leggett, R.; Lloyd, D.; Phipps, A.; Scott, B. *J. Radiol. Prot.* **2007**, *27*, 17.
(3) Greenwood, N.; Earnshaw, A. *Chemistry of the Elements*; Butterworth: Oxford, 1997.
(4) Richens, D. *The Chemistry of Aqua Ions*; Wiley: Chichester, U.K., 1997.
(5) Marcus, Y. *Ion Solvation*; Wiley: Chichester, U.K., 1986.
(6) Ohtaki, H.; Radnai, T. *Chem. Rev.* **1993**, *93*, 1157.
(7) Tomasi, J.; Persico, M. *Chem. Rev.* **1994**, *94*, 2027.
(8) Sanchez Marcos, E.; Pappalardo, R. R.; Rinaldi, D. *J. Phys. Chem.* **1991**, *95*, 8928.
(9) Consentino, U.; Villa, A.; Pitea, D.; Moro, G.; Barone, V. *J. Phys. Chem. B* **2000**, *104*, 8001.
(10) Martinez, J. M.; Pappalardo, R. R.; Sanchez Marcos, E.; Mennucci, B.; Tomasi, J. *J. Phys. Chem. B* **2002**, *106*, 1118.
(11) Becke, A. *J. Chem. Phys.* **1993**, *98*, 5648.
(12) Stephens, P. J.; Devlin, F. J.; Chabalowski, C. F.; Frisch, M. J. *J. Phys. Chem.* **1994**, *98*, 11623.
(13) Gill, P. M. W. *Mol. Phys.* **1996**, *89*, 433.
(14) Adamo, C.; Barone, V. *J. Comput. Chem.* **1998**, *19*, 419.
(15) Lee, C.; Yang, W.; Parr, R. G. *Phys. Rev. B* **1988**, *37*, 785.
(16) Miehlich, B.; Savin, A.; Stoll, H.; Preuss, H. *Chem. Phys. Lett.* **1989**, *157*, 200.
(17) Adamo, C.; Barone, V. *J. Chem. Phys.* **1998**, *108*, 664.
(18) Frisch, M. J.; Trucks, G. W.; Schlegel, H. B.; Scuseria, G. E.; Robb, M. A.; Cheeseman, J. R.; Montgomery, J. A., Jr.; Vreven, T.; Kudin, K. N.; Burant, J. C.; Millam, J. M.; Iyengar, S. S.; Tomasi, J.; Barone, V.; Mennucci, B.; Cossi, M.; Scalmani, G.; Rega, N.; Petersson, G. A.; Nakatsuji, H.; Hada, M.; Ehara, M.; Toyota, K.; Fukuda, R.; Hasegawa, J.; Ishida, M.; Nakajima, T.; Honda, Y.; Kitao, O.; Nakai, H.; Klene, M.; Li, X.; Knox, J. E.; Hratchian, H. P.; Cross, J. B.; Bakken, V.; Adamo, C.; Jaramillo, J.; Gomperts, R.; Stratmann, R. E.; Yazyev, O.; Austin, A. J.; Cammi, R.; Pomelli, C.; Ochterski, J. W.; Ayala, P. Y.; Morokuma, K.; Voth, G. A.; Salvador, P.; Dannenberg, J. J.; Zakrzewski, V. G.; Dapprich, S.; Daniels, A. D.; Strain, M. C.; Farkas, O.; Malick, D. K.; Rabuck, A. D.; Raghavachari, K.; Foresman, J. B.; Ortiz, J. V.; Cui, Q.; Baboul, A. G.; Clifford, S.; Cioslowski, J.; Stefanov, B. B.; Liu, G.; Liashenko, A.; Piskorz, P.; Komaromi, I.; Martin, R. L.; Fox, D. J.; Keith, T.; Al-Laham, M. A.; Peng, C. Y.; Nanayakkara, A.; Challacombe, M.; Gill, P. M. W.; Johnson, B.; Chen, W.; Wong, M. W.; Gonzalez, C.; Pople, J. A. *Gaussian 03*, revision D.01; Gaussian, Inc.: Wallingford, CT, 2004.
(19) Bylaska, E. J.; de Jong, W. A.; Kowalski, K.; Straatsma, T. P.; Valiev, M.; Wang, D.; Aprà, E.; Windus, T. L.; Hirata, S.; Hackler, M. T.; Zhao, Y.; Fan, P.-D.; Harrison, R. J.; Dupuis, M.; Smith, D. M. A.; Nieplocha, J.; Tipparaju, V.; Krishnan, M.; Auer, A. A.; Nooijen, M.; Brown, E.; Cisneros, G.; Fann, G. I.; Früchtl, H.; Garza, J.; Hirao, K.; Kendall, R.; Nichols, J. A.; Tsemekhman, K.; Wolinski, K.; Anchell, J.; Bernholdt, D.; Borowski, P.; Clark, T.; Clerc, D.; Dachsel, H.; Deegan, M.; Dyall, K.; Elwood, D.; Glendening, E.; Gutowski, M.; Hess, A.; Jaffe, J.; Johnson, B.; Ju, J.; Kobayashi, R.; Kutteh, R.; Lin, Z.; Littlefield, R.; Long, X.; Meng, B.; Nakajima, T.; Niu, S.; Pollack, L.; Rosing, M.; Sandrone, G.; Stave, M.; Taylor, H.; Thomas, G.; van Lenthe, J.; Wong, A.; Zhang, Z. *NWChem: A Computational Chemistry Package for Parallel Computers*, version 5.0; Pacific Northwest National Laboratory: Richland, WA, 2006.
(20) Schreckenbach, G.; Hay, P.; Martin, R. L. *Inorg. Chem.* **1998**, *37*, 4442.
(21) Schreckenbach, G.; Hay, P.; Martin, R. L. *J. Comput. Chem.* **1999**, *20*, 70.
(22) Schultz, N.; Zhao, Y.; Truhlar, D. G. *J. Phys. Chem. A* **2005**, *109*, 4388.
(23) Schultz, N.; Zhao, Y.; Truhlar, D. G. *J. Phys. Chem. A* **2005**, *109*, 11127.
(24) Dunning, T. *J. Chem. Phys.* **1989**, *90*, 1007.
(25) Peterson, K. A.; Figgen, D.; Goll, E.; Stoll, H.; Dolg, M. *J. Phys. Chem.* **2003**, *119*, 11113.
(26) Boys, S. F.; Bernardi, F. *Mol. Phys.* **1970**, *19*, 553.
(27) Simon, S.; Duran, M.; Dannenberg, J. J. *J. Chem. Phys.* **1996**, *105*, 11024.
(28) Cances, M.; Mennucci, B.; Tomasi, J. *J. Chem. Phys.* **1997**, *107*, 3032.
(29) Mennucci, B.; Tomasi, J. *J. Chem. Phys.* **1997**, *106*, 5151.
(30) Mennucci, B.; Cances, E.; Tomasi, J. *J. Phys. Chem. B* **1997**, *101*, 10506.
(31) Tomasi, J.; Mennucci, B.; Cances, E. *J. Mol. Struct. (THEOCHEM)* **1999**, *464*, 211.
(32) Zhan, C.-G.; Dixon, D. *J. Phys. Chem. A* **2004**, *108*, 2020.
(33) Martinez, J. M.; Pappalardo, R. R.; Sanchez Marcos, E. *J. Phys. Chem. A* **1997**, *101*, 4444.
(34) Amovilli, C.; Mennucci, B. *J. Phys. Chem. B* **1997**, *101*, 1051.
(35) Mennucci, B.; Martinez, J. M. *J. Phys. Chem. B* **2005**, *109*, 9818.
(36) Claverie, P.; Daudey, J. P.; Langlet, J.; Pullman, B.; Piazzola, D.; Huron, M. J. *J. Phys. Chem.* **1978**, *82*, 405.
(37) Tomasi, J.; Mennucci, B.; Cammi, R. *Chem. Rev.* **2005**, *105*, 2999.
(38) Tunega, D.; Hebrhauer, G.; Gerzabek, M.; Lischka, H. *J. Phys. Chem. A* **2000**, *104*, 6824.
(39) Lide, D. R. *CRC Handbook of Chemistry and Physics*; Taylor and Francis: Boca Raton, FL, 2006.
(40) Bukowski, R.; Szalewicz, K.; Groenenboom, G. C.; van der Avoird, A. *Science* **2007**, *315*, 1249.
(41) Feller, D.; Peterson, K. A. *J. Chem. Phys.* **2007**, *126*, 114105.
(42) Bak, K. L.; Jorgensen, P.; Olsen, J.; Helgaker, T.; Klopper, W. *J. Chem. Phys.* **2000**, *112*, 9229.
(43) Marcus, Y. *Chem. Rev.* **1988**, *88*, 1475.
(44) Martinez, J. M.; Hernandez-Cobos, J.; Saint-Martin, H.; Pappalardo, R. R.; Ortega-Blake, I.; Sanchez Marcos, E. *J. Chem. Phys.* **2000**, *112*, 2339.
(45) Glendening, E. D. J.; Badenhoop, K.; Reed, A. E.; Carpenter, J. E.; Bohmann, J. A.; Morales, C. M.; Weinhold, F. *NBO 5.0*; Theoretical Chemistry Institute, University of Wisconsin, Madison: Madison, WI, 2001.